

Snow ablation modelling in a mature aspen stand of the boreal forest

J. P. Hardy,^{1*} R. E. Davis,¹ R. Jordan,¹ W. Ni² and C. E. Woodcock²

¹*US Army Cold Regions Research and Engineering Laboratory, Hanover, NH, USA*

²*Department of Geography, Boston University, Boston, MA, USA*

Abstract:

Snow ablation modelling at the stand scale must account for the variability in snow cover and the large variations of components of energy transfer at the forest floor. Our previous work successfully predicted snow ablation in a mature jack pine stand by using a one-dimensional snow process model and models predicting radiation below forest canopies. This work represents a second test of our basic modelling scenario by predicting snow ablation in a leafless, deciduous aspen stand and verifying the results with field data. New modifications to the snow model accounted for decreased albedo owing to radiation penetration through optically thin snowpacks. A provisional equation estimates litter fall on the snowpack, thereby reducing the areal averaged albedo. We showed that subcanopy radiation measurements can be used with a canopy model to estimate a branch area index for defoliated aspen as an analogue to the foliage area index used for conifers. Modelled incoming solar and long-wave radiation showed a strong correlation with measurements, with $r^2 = 0.96$ and 0.91 for solar and long-wave radiation, respectively. Model results demonstrate that net radiation overwhelms turbulent exchanges as the most significant driving force for snowmelt in aspen forests. Predicted snow ablation in the aspen stand compared very favourably with available data on snow depth. © 1998 John Wiley & Sons, Ltd.

KEY WORDS snow ablation; boreal forest; aspen stand; snow model

INTRODUCTION

Preliminary predictions based on climate models suggest that the boreal regions of interior, western Canada are among the most sensitive areas in the world to the warming responses of greenhouse gases (Manabe and Wetherald, 1986). According to Bonan *et al.* (1992), continental warming, and the associated reduction in vegetation height, would result in a large increase in winter albedo and dramatic decreases in the air temperature of the northern high latitudes. The boreal forest represents 77% of the total forested area in Canada (Jones, 1987), and remains snow covered for six to eight months of the year. The Boreal Ecosystems–Atmosphere Study (BOREAS) is a large-scale, multidisciplinary project focused on understanding how the boreal ecosystem would respond to a change in climate (cf. Sellers *et al.*, 1995). BOREAS investigators conducted intensive field studies between 1993 and 1996 in the boreal forest of central Saskatchewan and northern Manitoba, Canada. Two BOREAS test areas, which bracket the range of annual temperature and precipitation in the central boreal forest, were selected for detailed modelling studies

*Correspondence to: Ms J. P. Hardy, US Army Cold Regions Research and Engineering Laboratory, 72 Lyme Road, Hanover, NH 03755, USA.

Contract grant sponsors: NASA; US Army.

Contract grant numbers: POS-12856-F, ref. 2250-BOREAS-U150; 4A762784AT42.

(Sellers *et al.*, 1995). In the south, the modelling subarea occupies 2000 km² and is composed of 55% conifer cover and 6% deciduous cover. In the north, the modelling subarea occupies 1200 km², with 40% of the area covered by evergreen conifer forest and 8% by deciduous hardwood forest. Our contributions to BOREAS are to develop models that will predict spatial distributions of snow properties and processes important to the hydrology of the area and the remote sensing signatures from snow-covered boreal scenes. These properties include depth, density, grain size and melting rate and are important for the estimation of the volume and timing of snowmelt.

In this paper we extended our approach for modelling snow ablation in a boreal jack pine forest (Hardy *et al.*, 1997) to another boreal forest ecosystem, mature aspen forest, and verify the models using field data. We apply the geometric-optical radiative transfer model, which describes radiation interactions with the forest canopy (Li *et al.*, 1995; Ni *et al.*, 1997), to a deciduous forest for the first time and use the results to drive radiation inputs to a one-dimensional snow process model (Jordan, 1991) newly modified for forested conditions and optically thin snow. This paper represents the second test of our basic modelling scenario with a long-term goal of spatially distributing snow in forested environments. Because spatially distributed modelling requires successful stand-scale modelling in a range of conditions, this work makes progress towards that goal by applying our methods to a new forest type.

PRIOR WORK

Forests are well known to alter the accumulation of snow on the ground and to modify near-surface micrometeorology, which controls snowmelt rates. Tree species and forest structure affect the distribution of snow on the forest floor (Golding and Swanson, 1986; Hardy and Hansen-Bristow, 1990; Hedstrom and Pomeroy, 1998). In conifer forests, tree wells develop around the stems during winter when the canopy intercepts incoming snow, which results in its depletion beneath the tree crown. Sturm (1992) observed snow cones at tree trunks around leafless deciduous trees, resulting from a combination of snow settling away from the trunk and snow sloughing off the branches. The net effect of forest canopies is a snowpack with spatially heterogeneous depth and snow water equivalence (SWE). Since physical models of snow interception by the tree canopies and subsequent sublimation, melt or mechanical removal are very recent (e.g. Hedstrom and Pomeroy, 1998) we focus our efforts on modelling snow ablation.

Radiation dominates the snow surface energy exchange during snow ablation in boreal conifer forests (Price and Dunne, 1976; Metcalfe and Buttle, 1995; Harding and Pomeroy, 1996; Hardy *et al.*, 1997). Hendrie and Price (1979) and Price (1988) showed that under leafless deciduous canopies the net radiation alone was a good predictor of snow ablation and the turbulent contribution to melt was minimal. Metcalfe and Buttle (1995) observed that a single measure of net radiation was inadequate to estimate snowmelt using the energy balance approach when modelling the influence of canopy structure on snowmelt in the boreal forest. We validate our canopy model predictions with measurement from several sensors. Barry *et al.* (1990) empirically adjusted the densification, metamorphism and liquid water retention algorithms of Anderson's (1976) energy and mass balance model to predict snow processes in a balsam fir forest. His work was based on point measurements of incoming solar, reflected solar and net all-wave radiation. We use a physically based model of snow. Other investigators used canopy properties in models to predict the amount of radiation reaching the snowpack, or snowmelt rates (Yamazaki and Kondo, 1992; Metcalfe and Buttle, 1995; Pomeroy and Dion, 1996). They generally found that as canopy density or tree height increases, radiation and snowmelt rates decrease. Yamazaki and Kondo (1992), coupling a two-layer canopy and snowmelt model, found that under some conditions, snowmelt increased under a dense canopy owing to decreased terrestrial radiative losses. Davis *et al.* (1997) showed the effect of both canopy and tree height on modelling energy budgets in boreal coniferous forest and the importance of solar radiation in these forests.

Our goal in modelling snow ablation and energy exchanges at the stand scale is to incorporate as much process-level detail as possible at a high (hourly) temporal resolution. Successful physically based modelling at the stand scale in the boreal forest is a necessary step towards spatially distributed modelling. Boreal forest

landscapes are a mixture of conifer and deciduous forest stands and to be able to do landscape-scale or drainage basin-scale modelling we need to be able to apply our scenario to both coniferous and deciduous forests.

METHODS

We modelled subcanopy radiation, turbulent transfer and snow processes at a leafless aspen site. The results were validated with field measurements.

Site description and BOREAS measurements

Data collection for this study focused on a stand of mature aspen (*Populus tremuloides*) north of Prince Albert, Saskatchewan (53.9° N, 104.7° W). This site is within Prince Albert National Park and is part of the southerly study area (SSA) of the BOREAS experiment. The forest understorey consists of hazelnut (*Corylus comuta*) and wildrose (*Rosa woodsii*). The mean annual air temperature near this site is 0.1 °C. The aspen site consists of 60-year-old trees of relatively uniform height (21.5 m). At the aspen site, Shewchuk (1997) measured standard meteorological variables and soil temperature continuously, reporting 15-minute averages (Table I). Additional data from BOREAS used in this work include stand characteristics (canopy closure, stem density and tree height) and biweekly snow survey data (snow depth, density and water equivalence) (Halliwell and Apps, 1997).

Field measurements of subcanopy meteorology and snow

Our field campaign occurred between 4 and 8 March 1996. At that time, an array of 10 Eppley pyranometers (0.3–3.0 µm wavelength) and two Eppley pyrgeometers (8–50 µm wavelength) were randomly placed on the snow surface in the forest stand to measure incoming solar irradiance for validation of our predictions of solar transmission and long-wave radiation. The radiometers each sat on a small box to provide stability on the snow surface and the instrument level was checked every two days. Resulting from the random placement, some radiometers were adjacent to a tree stem while others were located in small forest openings. Other subcanopy meteorological measurements during the four days consisted of 2.0 m wind speed and direction, 2.0 m air temperature and relative humidity collected from a portable tower near the radiometer array. We used a RM Young wind sensor with a 0.5 ms⁻¹ start-up speed to measure wind speed and direction. We used a Vaisala probe for temperature and relative humidity. A Campbell Scientific CR10 datalogger measured all parameters every 10 seconds and stored them as one minute averages.

Snow depth was measured and monitored in three different ways. First, an ultrasonic depth sensor measured snow depth from a single point in a forest opening at the study site. This depth gauge measured the distance from the sensor to the snow surface and provided a continuous record of snow depth for validation

Table I. Meteorological variables measured by Saskatchewan Research Council at the mature aspen site. Sensors are on a 37 m tower near the centre of the site. Tree heights are approximately 21.5 m

Variables measured	Height (m)	Accuracy	Sensor
Air temperature	23.7	±0.4 °C	Vaisala HMP35C
Within-canopy temperature	4.0	±0.25 °C	Campbell Scientific 107F
Relative humidity	23.7	±3%	Vaisala HMP35C
Wind speed and direction	23.7	5%, 2°	RM Young wind monitor
Precipitation	N/A	5%	Belfort gauge
Snow depth	15.0	±0.01 m	Campbell Scientific UDG1
Incident solar radiation	23.7	5%	Eppley pyranometer
Reflected solar radiation	23.7	5%	Eppley pyranometer
Incoming terrestrial radiation	36.8	2%	Eppley pyrgeometer
Soil temperature	-0.1, -0.2, -0.5	±0.4 °C	Campbell Scientific 107BAM

of our model runs (Shewchuk, 1997). Secondly, we made measurements of snow depth, SWE and snow pack properties at the study site during our field campaign in early March. We measured the snow depth variability using 100 randomly located measurements. To initialize the snow model, we measured a snow density profile at 0.03 m vertical resolution using a 100 cm³ density cutter and an electronic balance (accurate to ± 0.1 g). A Canadian snow sampler obtained depth-integrated density and SWE at nine random locations. We measured snow temperatures with dial stem thermometers and used a sieve set to estimate grain size distribution. Thirdly, BOREAS snow survey teams measured snow depth and SWE in a mature aspen forest near the study site. Snow surveys, conducted biweekly by BOREAS investigators near the main test area, provided a time-series of average depth, SWE and standard deviations. The snow survey was located 25 km north of the aspen stand where we collected data for the models. The site was selected to represent a mature aspen forest in the SSA and is similar to the forest at our study site. The snow course consists of five stations, 100 m apart, running along a south to north transect through the aspen forest. Every two weeks the snow survey team measured a depth-integrated SWE and density at every station. The snow survey team also measured snow depth ($n = 10$) at equally spaced locations along the transect. These data were averaged and the depths, SWE and standard deviations were reported.

Models

The energy flux at the surface (I , positive downwards) is composed of radiative, turbulent and convective exchanges

$$I = R_S \downarrow (1 - \alpha) + R_L \downarrow + R_L \uparrow + I_{\text{sen}} + I_{\text{lat}} + I_{\text{conv}} \quad (1)$$

where $R_S \downarrow$ is the energy flux of downwelling solar radiation, α is the snow albedo, $R_L \downarrow$ and $R_L \uparrow$ are the energy fluxes of downwelling and upwelling long-wave radiation, I_{sen} and I_{lat} are the turbulent fluxes of sensible and latent heat, respectively, and I_{conv} is heat convected by rain or falling snow. All units are in W m^{-2} .

We used physical models to describe the transmission of solar radiation through the canopy, the incoming long-wave radiation beneath the canopy, the snow surface energy exchange and the snow pack properties. Figure 1 summarizes the input and output variables and data flow of the two main models used in this study. A hybrid geometrical optical radiative transfer (GORT) model predicted the transmission of incoming solar radiation ($R_S \downarrow$) to the snow and canopy factors that we used to estimate incoming long-wave radiation ($R_L \downarrow$). We used the Stefan–Boltzmann equation with the canopy factors to predict $R_L \downarrow$. We used an empirical model to estimate wind speed near the snow surface. These variables, along with measurements of air temperature, humidity and precipitation, were used to drive the snow model SN THERM (Jordan, 1991).

Geometrical optical radiative transfer model. Li *et al.* (1995) developed the hybrid geometrical optical radiative transfer (GORT) model to estimate the solar radiation reflected from and transmitted within and below discontinuous vegetation canopies. The model evolved from reflectance models of forest canopies based on geometrical optics (Li and Strahler, 1986, 1992), in which the primary factor influencing the reflectance from a forest canopy is the three-dimensional geometry of trees and their proximity. The current GORT model incorporates a radiative transfer component to account for the contribution of multiple scattering within and between crowns (Li *et al.*, 1995) and, when necessary, the horizontal branching structure within crowns (Ni *et al.*, 1997). The full hybrid GORT model allows calculation of all solar radiation components (absorption, transmission and reflectance) both below the canopy and within the canopy as a function of height. GORT requires measurements or estimates of above-canopy direct and diffuse solar radiation as well as forest stand variables. Modification of the original GORT model (which was developed to estimate the reflectance characteristics of forest canopies) for use in estimating transmission, and tests in a jack pine stand were reported by Ni *et al.* (1997). The effect of incorporating the transmission estimates from GORT on snowmelt in that stand was reported by Hardy *et al.* (1997).

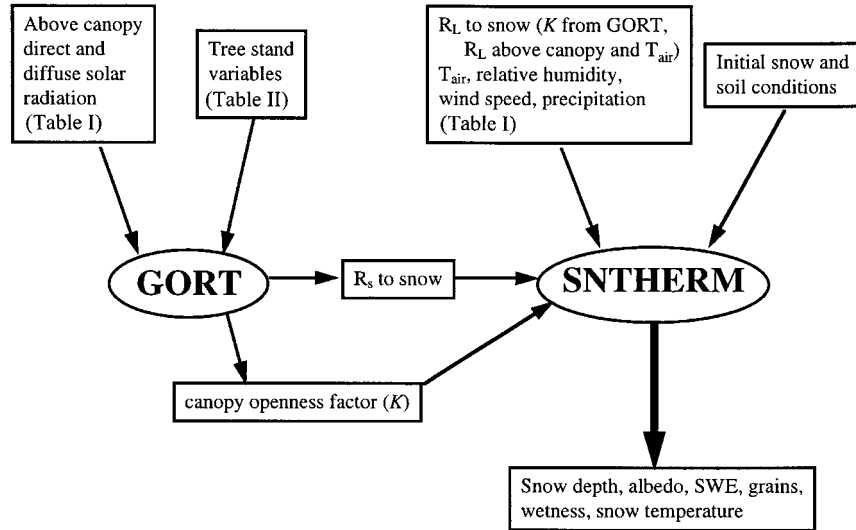


Figure 1. Input and output variables and data flow for the two primary models used in this study, GORT and SNTHERM

Table II. Parameters used by GORT for characterization of tree geometry and radiative properties at the mature aspen stand: b/R is the ratio of the vertical crown radius (b) to horizontal crown radius (R)

Parameters	Aspen
Horizontal crown radius, R (m)	2.12
Vertical crown radius, b (m)	5.38
b/R	2.54
BAVD (m^{-1})	0.061
Stem density (stems m^{-2})	0.114
Tree height (m)	2.15

The forest parameters required for GORT include those characteristic of forest types and those specific to individual stands. For the aspen site we summarize these in Table II. Parameters specific to forest types include the ratio of vertical to horizontal crown radius and the branch (or foliage) area volume density (BAVD) (defined below). The BAVD (or FAVD) is related to the effective leaf area index (ELAI) after considering the geometry of the branches and a single crown. Parameters describing unique tree stands are the stem density (number of stems per unit area) and tree height, which are often available from forest inventories. We measured these parameters directly at the aspen site.

GORT models discontinuous vegetation canopies as an assemblage of many individual tree crowns of ellipsoidal shape, with a random distribution of trees. Within each crown the foliage and branches are assumed to be randomly distributed. The incoming direct and diffuse solar irradiance can pass through the gaps between crowns, and enter tree crowns at different heights, with some fraction both scattered and unscattered through gaps within the crowns. The solar radiation reaching the forest floor consists of contributions from unscattered beam, multiscattered beam and diffuse solar radiation. Increases in R and stem density reduce the gap probability between crowns, while increases in BAVD reduce the probability of a beam reaching the snow surface unscattered.

The greatest challenge of radiation modelling was applying the GORT model to the deciduous aspen stand in the leaf-off condition. Our previous use of this model had been with evergreen conifers where needles were

the dominant attenuators (Ni *et al.*, 1997). The dominance of needles in this regard is reflected in the use of the term 'foliage' area volume density (FAVD) to describe the density of attenuating material in a canopy, when in fact this parameter also includes the density of the woody material in the canopy. However, in the case of aspen stands in the winter when they have dropped their leaves, branches and twigs become the dominant attenuators. To apply the GORT model in this situation, it was necessary to incorporate a 'branch' area volume density, or BAVD. Initially, we were unaware of field measurements to calibrate this parameter, so the GORT model was run with a range of BAVD values to fit predictions of solar transmission with measurements. Later, field measurements were located from another study (P. Blanken, personal communication), providing a measure of BAVD for the aspen stand.

Downwelling terrestrial irradiance at the forest floor was calculated from the relative contributions from the atmosphere and tree canopy

$$R_{L(\text{for})\downarrow} = R_{L(\text{open})\downarrow}(K_{\text{btw}} + K_{\text{in}}) + [1 - (K_{\text{btw}} + K_{\text{in}})]\varepsilon\sigma T^4 \quad (2)$$

where K_{btw} is canopy openness as determined between the crowns, K_{in} is the openness through the crowns, ε is the canopy emissivity (0.98), T is the canopy temperature and σ is the Stefan–Boltzmann constant ($5.67 \times 10^{-8} \text{ W m}^{-2} \text{ K}^{-4}$). K_{btw} is GORT derived as the proportion of hemispherically isotropic sky light that hits the snow surface unscattered, by passing through gaps in the canopy. The variable K_{in} is also GORT derived as the proportion of hemispherically isotropic sky light that passes through the crowns and hits the snow surface unscattered. Hence, $K_{\text{btw}} + K_{\text{in}}$ is the total hemispherical openness in the stand. We assumed the canopy temperature was equal to the 4.0 m air temperature measured on the tower.

Snow process and energy budget model. SNTHERM is a one-dimensional mass and energy balance model for predicting snowpack properties and processes (Jordan, 1991), and forms the foundation for the snow modelling effort. SNTHERM calculates energy exchange at the surface and bottom of the snow cover, in-pack processes, grain growth, densification and settlement, melting and liquid water flow, heat conduction and vapour diffusion (Jordan, 1991). The model has compared favourably with measurements at sites ranging from seasonal snow (Jordan, 1991; Harrington *et al.*, 1995) to polar snow (Rowe *et al.*, 1995). SNTHERM was developed and validated for open snow fields and was first applied to a conifer forest by Hardy *et al.* (1997) and Davis *et al.* (1997). This is its first known application to a deciduous forest.

Measured incident radiation above the canopy provided input for the GORT model (described above), which in turn predicted subcanopy radiation incident to the snow surface. Solar radiation attenuates exponentially within the snowpack as described in Koh and Jordan (1995). SNTHERM computes reflected solar radiation using an albedo routine that accounts for changes in albedo resulting from grain growth, sun angle and cloud cover (Marks, 1988). Preliminary model runs of SNTHERM in the aspen site suggested a lower albedo than predicted by SNTHERM during late season ablation. This phenomenon was also observed in modelling snow ablation in the jack pine forest (Hardy *et al.*, 1997). To address this problem, we built in a routine to reduce albedo automatically when radiation penetrates through the snowpack to the underlying soil. This algorithm for optically thin snow uses the spectral albedo equation of Choudhury and Chang (1979), but lumps incident short-wave radiation into two broad spectral bands with wavelength ranges of 0.4–0.7 μm and 0.7–2.4 μm (see Appendix). The algorithm is limited to clear, dry snow conditions and diffuse, incident irradiance but is applicable to a range of snow densities and grain sizes. For example, Figure 2 shows the spectrally integrated albedo and our bulk formulation as a function of snow depth for new and old snow characterized by snow densities and grain sizes of 80 and 350 kg m^{-3} and 0.2 and 3.0 mm, respectively. Computed albedo is 5% below its semi-infinite (deep snowpack) value at snow depths of 0.07 and 0.15 m for new and old snow, respectively. The optically thin snow correction is thus a function of optical depth and grain size, and for older snow, significantly reduces albedo for depths less than 0.1 to 0.15 m, trending towards the soil albedo (0.2) as depth reduces.

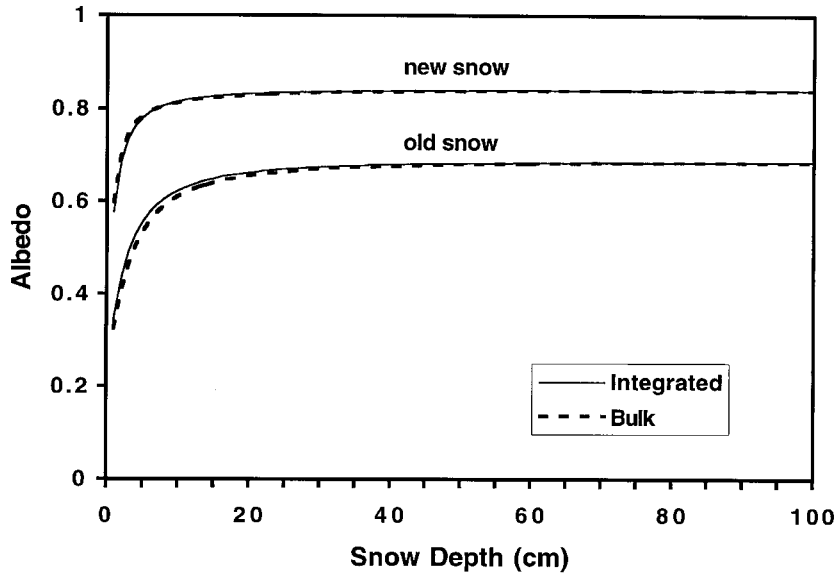


Figure 2. Comparison of Choudhury and Chang's (1979) spectrally integrated albedo (solid line) and our bulk formulation (dashed line) as a function of snow depth

The snow correction described above assumes clean snow, free of forest litter. As this situation is unlikely beneath an aspen stand, we therefore include a provisional routine to estimate litter fall on the forest floor, thereby reducing the subcanopy snow albedo as forest litter accumulates (Oke, 1987; Pomeroy and Dion, 1996). The fraction of litter in or on the snow pack was increased throughout the entire snow season according to Equation (3)

$$lc = 1.0 - (1.0 - lr)^{\text{day}} \quad (3)$$

where lc is the fractional litter coverage ($\text{m}^2 \text{m}^{-2}$) and lr is the daily litter rate ($\text{m}^2 \text{m}^{-2} \text{d}^{-1}$). The resulting albedo is a weighted average of litter albedo and clean snow albedo in proportion to their areal coverage.

Litter accumulates on the snow surface beginning with the first snowfall. Since our model run begins at peak accumulation, the litter contents of the initial snow layers were computed by Equation (3) based on the number of days between snow events, leading to the maximum accumulation. We assumed a litter rate of 0.001d^{-1} for the aspen site. The albedo of the aspen litter (0.2) was based on the results of Oke (1987). The number of days when snow was on the ground in the aspen site was 159 days. There are two ways in which the fraction of litter on the snow surface can increase. Either existing snow layers melt, leaving behind their litter on the snow surface, or additional litter accumulates on the snow surface through time. The litter equation estimates a total litter coverage of 15% in the aspen forest at the end of the snow ablation period.

This litter routine is a preliminary attempt at considering the well-known effect litter has on reducing albedo. Unfortunately, we know of no data collected on litter fall in a deciduous forest during the snow season and the effect of wind on litter accumulation on the snow surface is not yet considered. Future work will be aimed at developing a physically based algorithm that will incorporate litter data and wind measurements.

Measurements of subcanopy wind speed for four days provided sufficient data to develop the following expression for estimation of wind speeds in the aspen stand from above-canopy measurements

$$ws_{\text{for}} = \max[(ws_{\text{above}} 0.27) - 0.24, 0] \quad (4)$$

where ws_{for} is the subcanopy wind speed (m s^{-1}) and ws_{above} is the wind speed (m s^{-1}) above the canopy.

Model initial conditions. The snow model SNTHERM provided information on the average energy fluxes and snow depth variations, incorporating accumulation, ablation, compaction and evaporation for the stand. We ran the models from approximately the time of peak SWE (day 61) until complete ablation (day 132). We initialized the model run with soil temperatures from measurements at depths of 0.1, 0.2 and 0.5 m and field measurements of snow depth, density, temperature and grain size. Turbulent fluxes were computed by SNTHERM using values of 0.005 m and $1.0 \text{ W m}^{-2} \text{ K}^{-1}$ for the roughness length and windless exchange coefficient for sensible heat, respectively. The latter provides sensible heat transfer at the surface even when mean wind speeds are near zero and the standard stability correction exceeds the critical Richardson number for exchange in stable stratification (Jordan, 1991). We assumed that the roughness lengths for momentum, heat and water vapour were equal.

Snow properties used to initialize SNTHERM were derived from a combination of *in situ* measurements on day 64 and data from the snow survey conducted on day 60. To initialize the snow density we used data from the snow survey ($n = 5$) that were an approximate mean of all available measurements. We input initial snow densities in 0.03 m intervals. Modelled snow depths were compared with continuous snow depth data from the ultrasonic depth sensor and biweekly snow survey data.

RESULTS

Solar and long-wave radiation

Meteorologically determined boundary conditions at the air interface and solar absorption within the snowpack were the primary driving factors under the aspen canopy. To a lesser extent, heat fluxes from the underlying soil affected heat exchange with the snowpack. Measured values of incoming solar radiation on the snow surface show high temporal and spatial variation at the aspen site (Figure 3) compared

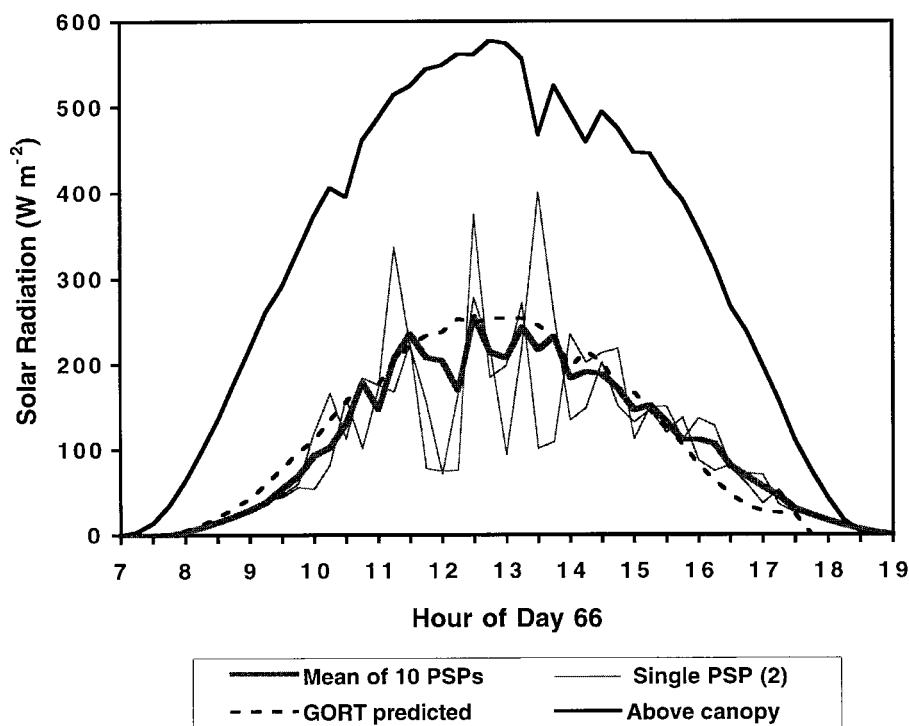


Figure 3. Measured data comparing above canopy $R_{S\downarrow}$ (thick black line) with subcanopy $R_{S\downarrow}$ measurements from two Eppley pyranometers (PSPs) (thin grey lines). Also shown for comparison is the mean value of 10 subcanopy PSPs (thick grey line) and the GORT-predicted subcanopy $R_{S\downarrow}$ (dashed line). All data and the GORT model simulation are for day 66, 1996

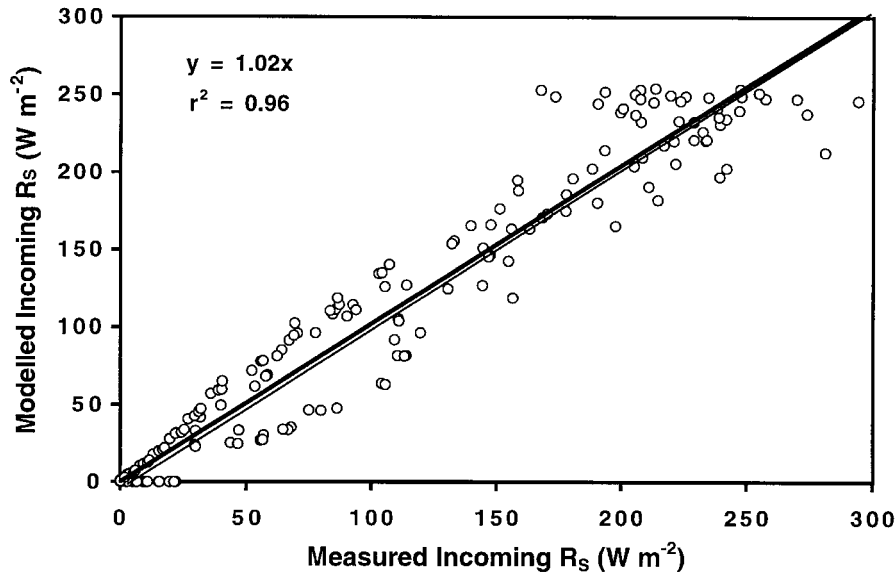


Figure 4. GORT modelled vs. measured subcanopy $R_s \downarrow$ at the snow surface in the aspen stand. The thin line has a slope of 1. The thick line is the linear regression ($r^2 = 0.96$)

with incoming solar radiation above the canopy. In Figure 3 only data from two radiometers are shown to illustrate the inherent variability between measurements. This variability characterizes the sensitivity of patterns of radiation to species and other variables, such as canopy closure, tree and stand geometry. All data were collected during nearly clear-sky conditions in early March. The patterns of radiation measured beneath the aspen canopy (from all 10 radiometers) are characterized by peak irradiances of 500 W m^{-2} and maximum diffuse radiation less than 100 W m^{-2} . Iterations of the GORT model yielded an estimated BAVD of 0.065 m^{-1} for the aspen stand. This value agrees well with another study (P. Blanken, personal communication) where field measurements were used to estimate the BAVD of the aspen stand (0.061 m^{-1}). The fact that these two independent methods produced similar results was encouraging. We then compared the results of the modelled understory solar radiation with the field measurements collected in the aspen stand in early March 1996 (Figure 4). The goodness-of-fit for these data throughout the range of observed values is excellent ($r^2 = 0.96$). Interestingly, even without leaves, the transmission in aspen stands during the snowmelt season is surprisingly low. We measured transmission of solar radiation through the canopy at only 32% in early March at the highest sun angles. As sun angle decreases, so does transmission.

Next, we compared the measured vs. modelled incoming long-wave radiation at the snow surface in the aspen site (Figure 5). The measured long-wave radiation is the average of two pyrgeometers. The correlation between the measured data and the model results is strong ($r^2 = 0.91$), but the model underpredicts the incoming long-wave radiation by approximately 8 W m^{-2} .

Wind speed, turbulent and radiative fluxes

Our model for subcanopy wind speeds [Equation (4)], based on a least-squares regression of short-term measurements of winds above and below the canopy, yielded a relatively weak relationship ($r^2 = 0.42$). The very low wind speeds at the 2.0 m height in the aspen forest were often below the threshold of the RM Young wind sensor (0.5 m s^{-1}). The predicted subcanopy wind speeds ranged from 0 to only 1.8 m s^{-1} for the duration of the ablation season in the aspen site.

The SNTHERM output provides a time-series of turbulent and radiative exchanges during the late ablation period (day 100–125) in the aspen stand (Figure 6). Figure 6 shows the magnitude of the different

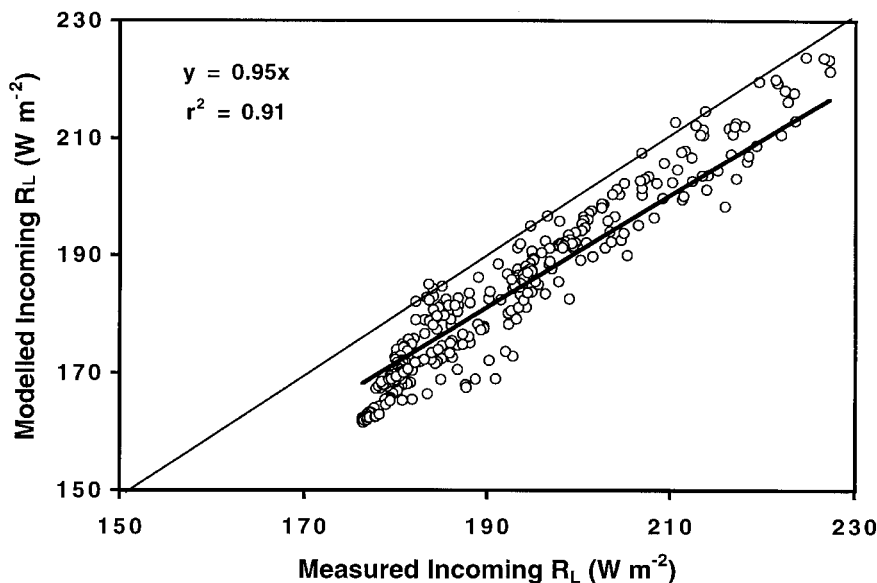


Figure 5. Modelled $R_L \downarrow$ on the snow surface vs. average measurements of two Eppley pyrgeometers in the aspen stand. The thin line has a slope of 1. The thick line is the linear regression ($r^2 = 0.91$)

components in the energy balance as predicted by SNTHERM. In the aspen stand, latent heat is negligible and sensible heat is positive, albeit small. The low wind speeds result in small turbulent fluxes, minimizing their contribution to the overall energy exchange in a forested environment. Net radiation overwhelms turbulent exchanges as the most significant driving force for snowmelt in leafless deciduous forests. The net energy is controlled by the solar component, which reinforces the need for accurate predictions of solar radiation beneath a canopy.

Snow depths

At peak accumulation in the aspen site, snow distribution patterns around the tree stems were different from those previously observed in coniferous sites. Tree wells were absent; an ablation hollow formed adjacent to the south side of the trunk, while the north side showed a slight cone of deeper snow. The average snow depth, based on 100 random measurements, was 0.38 m, with a standard deviation of 0.052 m and a range between 0.26 and 0.46 m. The mean snow depth from the snow survey on day 60 was 0.39 m, with a standard deviation of 0.037 m. The average snowpack density from our *in situ* measurements was higher than reported by the snow survey team (a discrepancy previously observed for the two different measurement techniques).

The modelled output for snow depth shows complete ablation in the aspen stand by day 124 (Figure 7). These model results are compared with a point measurement of snow depth measured continuously in the aspen forest and snow survey results from a similar mature aspen forest. The model run was initialized with a snow depth of 0.39 m. Vertical lines are standard deviations of depth from the snow survey measurements. The decrease in predicted snow depth early in the modelling period is a result of a compaction routine recently incorporated into SNTHERM. The snow sensor data do not exhibit this compaction. According to Sturm (1991), developed depth hoar is more resistant to compaction than snow of other textures with the same density. The snow at the start of the model run consisted entirely of depth hoar and faceted grains. Future modifications to the SNTHERM code will need to address this snow condition.

Data from the ultrasonic snow depth sensor agree well with the model prediction; however, the depth sensor suggests a higher ablation rate than predicted. To understand the behaviour of the depth sensor late in

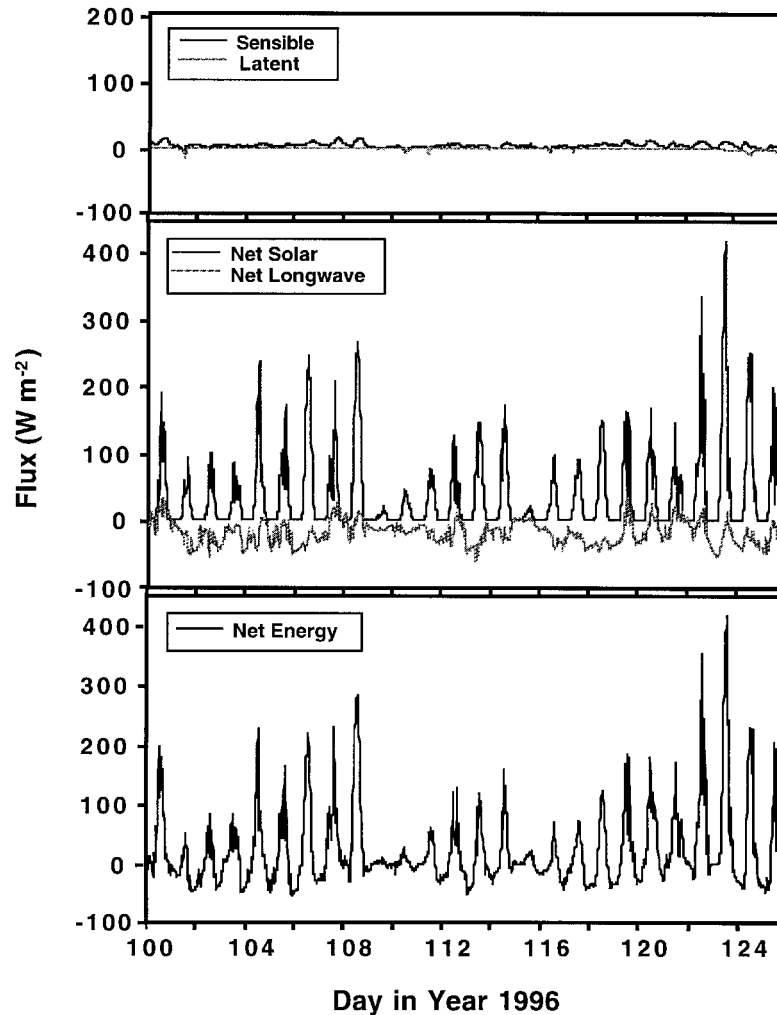


Figure 6. SNTHERM predicted energy fluxes at the snow surface for the ablation period between days 100–125, 1996

the ablation period (day 100 onwards), we plotted the measured, noontime, above-canopy albedo (Figure 8). The plotted albedo includes both the albedo of the snow and the aspen canopy. The low albedo on day 108 (0.1) corresponds to a measured snow depth of 0 m. Increases in albedo on days 109 and 116 correspond to snowfall events. On day 120 the measured albedo drops to, and remains at, 0.1, suggesting complete ablation of the snowpack, despite the presence of new snow 'measured' by the sensor. The absorption of solar energy by bare ground sends a different signal from snow and is known to affect the operation of the sensor negatively. Consequently, the data collected shortly after snow disappearance are 'noisy' and should be disregarded. On day 122, snow survey data show a remaining snow depth of 0.032 m (standard deviation 0.053 m). Overall, the model results compare favourably with available snow depth measurements.

DISCUSSION

Physically based modifications to SNTHERM improved its capability for predicting energy exchanges and snowpack properties and processes in aspen forests. These modifications take into consideration the ability

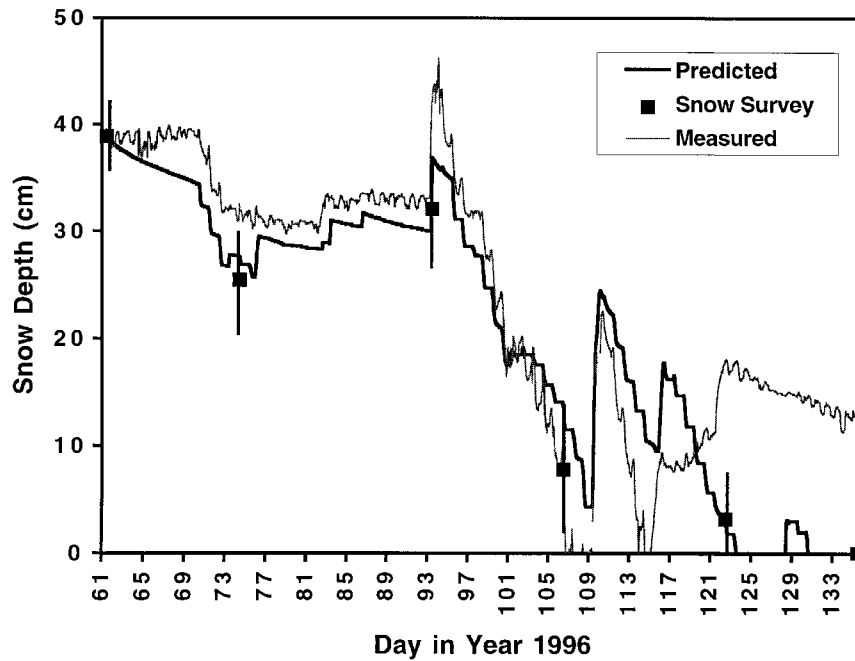


Figure 7. Model-predicted snow depth in the aspen stand for the ablation season (day 61–135). Model results are validated with a continuous point measurement of snow depth (grey line) and biweekly snow surveys from a similar aspen stand (solid squares). The vertical lines are standard deviations of depth from the snow survey measurements

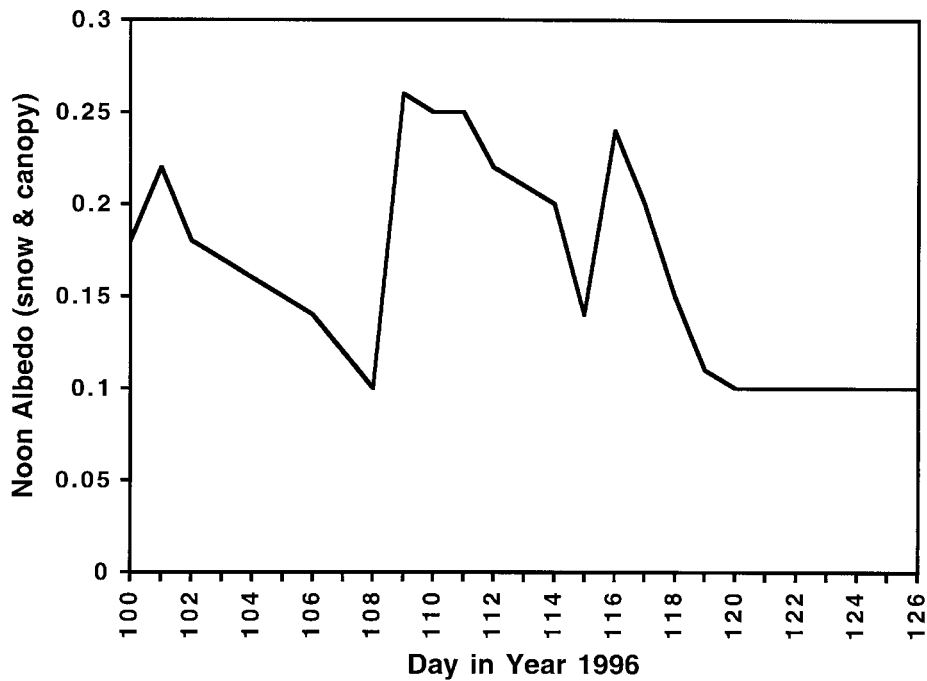


Figure 8. Above-canopy, noontime albedo of the aspen forest during snow ablation. The albedo of the snow and canopy goes to 0.1 when snow cover is absent

for radiation to penetrate optically thin snowpacks and thereby result in a lower albedo than would be expected for deep snow. With these new modification, the models SNTHERM and GORT, along with litter estimates and physically based meteorological adjustments, provided good estimates for the timing of snowmelt in mature aspen stands, especially considering the well-known variability of snow depth in forested environments. Modelled snow ablation agreed well with available measurements, but does suggest an apparent underestimation of the ablation rate (Figure 7) probably as a result of the albedo estimation. The albedo function in SNTHERM is based on the most widely accepted model for the spectral albedo of snow, but one that is also known to overestimate the albedo of old and melting snow (Wiscombe and Warren, 1980). A lower albedo than that predicted by SNTHERM would increase ablation rates. This work improved the albedo predictions for optically thin, melting snowpacks, but shows that more work is needed on deep snowpack albedo.

To address our model's underestimation of the incoming long-wave radiation at the snow surface, we recall that this model considers the relative long-wave contribution from both the sky (measured above the trees) and the canopy (GORT-derived openness factor, 4 m air temperature and Stefan–Boltzman equation). There are three considerations for evaluating the underestimation. First, the above-canopy pyrgeometer was factory-calibrated prior to installation and so not a likely source of error. Secondly, we are confident in the GORT-derived canopy openness factor (k) used in calculating long-wave because its use in calculating the transmitted radiation yielded close matches with measurements (Figure 4). Thirdly, we question our assumption that the 4.0 m air temperature represents effective radiant temperature of aspen branches and twigs. The 8 W m⁻² systematic model underestimation could be explained by a canopy and air temperature difference of about 4 °C. Our assumption of an equilibrium between canopy radiant temperature and air temperature requires further study.

The influence of trees on hydrological processes has important implications for distributed snowmelt modelling. For the boreal forest region of Canada, much of the necessary land cover data for running distributed canopy and snow models can be obtained from standard forest inventory maps, adjustments to these maps to account for non-productive treed areas, digital terrain models and soil maps. Recent results describing new algorithms for measuring snow cover fraction on a pixel by pixel basis (Rosenthal and Dozier, 1996) show promise for improved detection and mapping of snow in forests and canopy density mapping when the snow is continuous (e.g. Rosenthal, 1995). An improved understanding of the relationships between snow distribution and forest canopy (Hedstrom and Pomeroy, 1998) is also important to provide the information necessary for distributed snowmelt modelling.

CONCLUSIONS

Methods previously developed by us to model snow ablation in a boreal jack pine forest have now been successfully applied to a boreal aspen forest. The parameters (namely BAVD) required to run the GORT model required special consideration for the deciduous aspen application. A new modification to existing albedo controls in SNTHERM improved the model for this application, and we expect that it may be useful for other applications as well. The new modification reduced albedo for optically thin and litter-contaminated snowpacks. Individual components of the energy balance equation were modelled and our approach was shown to work especially well for the solar components. Some work is needed to improve our estimates of incoming long-wave radiation through a closer examination of the canopy radiant temperature. Modelled snow ablation agreed well with the available measurements in mature aspen forests and provided good estimates of the delivery of water to the soil system. The mass and energy transfer model for snow, SNTHERM, and the geometrical optical radiative transfer model for canopy, GORT, provided a sound, physically based approach to modelling snow ablation in deciduous forests. This approach will ultimately be coupled with remote sensing products to distribute snow properties and processes spatially throughout various ecosystems of the boreal region.

APPENDIX. ALBEDO ADJUSTMENT FOR OPTICALLY THIN SNOW

Using a modified Schuster–Schwartzschild two-stream approximation (Sagan and Pollack, 1967) as reported by Choudhury and Chang (1979), the spectral albedo of an optically thin snowpack is computed as

$$\alpha_\lambda = \frac{(\alpha_{\text{soil}}\alpha_\infty - 1)\alpha_\infty + (\alpha_\infty - \alpha_{\text{soil}}) e^{-2A\tau}}{(\alpha_{\text{soil}}\alpha_\infty - 1) + \alpha_\infty(\alpha_\infty - \alpha_{\text{soil}}) e^{-2A\tau}} \quad (\text{A1})$$

where α_{soil} is the albedo of the underlying soil, α_∞ is the spectral albedo of the semi-infinite snowpack

$$\alpha_\infty = 1 - \frac{2\sqrt{1-\omega}}{\sqrt{1-\omega} + 2\omega\beta + \sqrt{1-\omega}} \quad (\text{A2})$$

τ is the optical depth of the snow pack

$$\tau = \frac{3\rho_{\text{snow}}H}{2R\rho_{\text{ice}}} \quad (\text{A3})$$

and A is computed as

$$A = \sqrt{\frac{(1-\omega)(1-\omega+2\beta\omega)}{\delta}} \quad (\text{A4})$$

In Equation (A3), ρ_{snow} is the density of snow, ρ_{ice} is the density of ice, R is the grain radius and H is the depth of the snowpack. All units are in the mks system. In Equations (A2) and (A4), ω is the single scattering albedo

$$\omega = (1/2) + (1/2)\exp(-1.67k_\lambda R) \quad (\text{A5})$$

where k_λ is the absorption coefficient of ice for wavelength λ , computed from the imaginary index of refraction for ice n_{im} as $k_\lambda = 4\pi n_{\text{im}}/\lambda$. In the modified Schuster–Schwartzschild formulation, $\delta = 1/\sqrt{3}$ and $\beta = 0.065$. The spectrally integrated albedo in Figure 2 is computed by summing over the wavelength band of 0.4 to 2.4 μm in wavelength increments of 0.005 μm

$$\bar{\alpha}_{0.4-2.4} = \sum_{\lambda=0.4,2.4} f_\lambda \alpha_\lambda \quad (\text{A6})$$

where α_λ is the spectral albedo at the mid-point of the segment, computed from Equation (A1), and f_λ is the fraction of incident spectral irradiance in the segment, taken from the clear-sky curve of Grenville and Perovich (1984, their Figure 8).

In our approximation, we break the spectrum into two broad bands of 0.4–0.7 μm and 0.7–2.4 μm . A bulk albedo, $\bar{\alpha}$, is then computed from Equation (A1) for each band, by replacing α_∞ with bulk semi-infinite albedos $\bar{\alpha}_{\infty,0.4-0.7}$ and $\bar{\alpha}_{\infty,0.7-2.4}$, and computing A in Equation (A4) with bulk single scattering albedos $\bar{\omega}_{0.7-0.9}$ and $\bar{\omega}_{0.9-2.4}$, where

$$\bar{\omega}_{0.4-0.7} = 1 - 0.165R \quad \text{for } 0.4 < 1 \leq 0.7 \quad (\text{A7})$$

and

$$\bar{\omega}_{0.7-2.4} = (1/2) + (1/2)\exp(-42.R) \quad \text{for } 0.7 < 1 \leq 2.4 \quad (\text{A8})$$

We then estimated the optically thin albedo as

$$\bar{\alpha}_{\text{est}} = f_{\text{vis}} \bar{\alpha}_{\text{est}, 0.4-0.7} + (1 + f_{\text{vis}}) \bar{\alpha}_{\text{est}, 0.7-2.4} \quad (\text{A9})$$

Here, f_{vis} is the fraction of incident spectral irradiance in the visible waveband. The form of Equation (A7) derives from a first-order Taylor expansion of Equation (A5). The parameters 0.165 and 42 in Equations (A7) and (A8), respectively, provide a minimum RMS error of 0.0095 between the spectrally integrated and bulk albedo parameterizations for all combinations of the following snow characteristics and soil albedos: snow densities of 80 and 350 kg m⁻³, grain radii of 0.0001, 0.0005 and 0.0015 m, and soil albedos of 0.2 and 0.4. Our optimization procedure considers snow depths between 0.01 and 0.20 m at 0.01 m increments. Equation (A10) does not give good results when $\alpha_{\text{soil}} > \alpha_{\infty}$ or for low density, new snow with grain radii exceeding 0.0005 m.

ACKNOWLEDGEMENTS

Funding for this research was provided by NASA (grant no. POS-12856-F; reference no. 2250-BOREAS-U150) and supplemented by US Army Project 4A762784AT42. The authors thank Saskatchewan Research Council for meteorological data, B. Goodison's team for snow survey data and Prince Albert National Park personnel for their assistance. R. Kattelmann, B. Nijssen and B. Harrington helped ensure the collection of quality field data. We are grateful for the helpful comments by R. Melloh and M. Sturm of CRREL and two anonymous reviewers.

REFERENCES

- Anderson, E. A. 1976. 'A point energy and mass balance model of a snow cover', *NOAA Tech. Rep. NWS 19*. US Dept of Commerce, Silver Spring.
- Barry, R., Prevost, M., Stein, J., and Plamondon, A. P. 1990. 'Application of a snow cover energy and mass balance model in a balsam fir forest', *Wat. Resour. Res.*, **26**, 1079–1092.
- Bonan, G. B., Pollard, D., and Thompson, S. L. 1992. 'Effects of boreal forest vegetation on global climate', *Nature*, **359**, 716–718.
- Choudhury, B. J. and Chang, A. T. C. 1979. 'Two-stream theory of reflectance of snow', *IEEE Trans. Geosci. Electron.*, **17**, 63–68.
- Davis, R. E., Hardy, J. P., Ni, W., Woodcock, C., McKenzie, J. C., Jordan, R., and Li, X. 1997. 'Variation of snow cover ablation in the boreal forest: a sensitivity study on the effects of conifer canopy', *J. Geophys. Res.*, **102**, 29389–29396.
- Golding, D. L. and Swanson, R. S. 1986. 'Snow distribution patterns in clearings and adjacent forest', *Wat. Resour. Res.*, **22**, 1931–1940.
- Grenville, T. C. and Perovich, D. K. 1984. 'Spectral albedos of sea ice and incident solar irradiance in the Southern Beaufort Sea', *J. Geophys. Res.*, **89**, 3573–3580.
- Halliwell, D. H. and Apps, M. J. 1997. 'Boreal Ecosystem–Atmosphere Study (BOREAS) biometry and auxiliary sites: overstory and understory data', Natural Resources Canada, Canadian Forestry Centre, Edmonton, Alberta, 1997, 254 pp.
- Harding, R. J. and Pomeroy, J. W. 1996. 'The energy balance of the winter boreal landscape', *J. Climate*, **9**, 2778–2787.
- Hardy, J. P. and Hansen-Bristow, K. J. 1990. 'Temporal accumulation and ablation patterns in forests representing varying stages of growth', in *Proc. of the 58th Western Snow Conf. Sacramento, CA*, pp. 23–34.
- Hardy, J. P., Davis, R. E., Jordan, R., Li, X., Woodcock, C., Ni, W., and McKenzie, J. C. 1997. 'Snow ablation modelling at the stand scale in a boreal jack pine forest', *J. Geophys. Res.*, **102**, 29397–29406.
- Harrington, R. F., Elder, K., and Bales, R. C. 1995. 'Distributed snowmelt modeling using a clustering algorithm', in Tonnessen, K., Williams, M. W., and Tranter, M. (eds), *Biogeochemistry of Seasonally Snow-Covered Catchments*. Proc. Boulder Symp., July 1995, IAHS Publ. no. 228, pp. 167–174.
- Hedstrom, N. R. and Pomeroy, J. W. 1998. 'Accumulation of intercepted snow in the boreal forest: measurements and modelling', *Hydrol. Process.*, **12**, 1611–1625 (this issue).
- Hendrie, L. K. and Price, A. G. 1979. 'Energy balance and snowmelt in a deciduous forest', in Colbeck, S. and Ray, M. (eds), *Proc. Modelling of Snowcover Runoff*. US Army Cold Regions Res. Eng. Lab., Hanover, New Hampshire, pp. 211–221.
- Jones, H. G. 1987. 'Chemical dynamics of snowcover and snowmelt in a boreal forest', in Jones, H. G. and Orville-Thomas, J. (eds), *Seasonal Snowcovers: Physics, Chemistry, Hydrology*. D. Reidel Publ. Co., Boston, pp. 531–574.
- Jordan, R. 1991. 'A one-dimensional temperature model for a snow cover: technical documentation for NSTHERM.89', *Spec. Rep. 91-16*. US Army Corps of Eng., Cold Reg. Res. and Eng. Lab., Hanover, New Hampshire.
- Koh, G. and Jordan, R. 1995. 'Sub-surface melting in a seasonal snow cover', *J. Glaciol.*, **41**(139), 474–482.
- Li, X. and Strahler, A. H. 1986. 'Geometric-optical bidirectional reflectance modelling of a conifer forest canopy', *IEEE Trans. Geosci. Remote Sens.*, **24**, 906–919.

- Li, X. and Strahler, A. H. 1992. 'Geometric-optical bidirectional reflectance modelling of mutual shadowing effects of crowns in a forest canopy', *IEEE Trans. Geosci. Remote Sens.*, **30**, 276–292.
- Li, X., Strahler, A. H., and Woodcock, C. E. 1995. 'A hybrid geometric optical-radiative transfer approach for modelling albedo and directional reflectance of discontinuous canopies', *IEEE Trans. Geosci. Remote Sens.*, **33**, 466–480.
- Manabe, S. and Wetherald, R. T. 1986. 'Reduction in summer soil wetness induced by an increase in atmospheric carbon dioxide', *Science*, **232**, 626–628.
- Marks, D. 1988. 'Climate, energy exchange, and snowmelt in Emerald Lake Watershed, Sierra Nevada', *PhD Thesis*, University of California at Santa Barbara.
- Metcalfe, R. A. and Buttle, J. M. 1995. 'Controls of canopy structure on snowmelt rates in the boreal forest', in *Proc. of the 52nd Eastern Snow Conf., Toronto, Ont.* pp. 249–257.
- Ni, W., Li, X., Woodcock, C. E., Roujean, J. L., and Davis, R. E. 1997. 'Transmission of solar radiation in boreal conifer forests: measurements and models', *J. Geophys. Res.*, **102**, 29555–29566.
- Oke, T. R. 1987. *Boundary Layer Climates*, 2nd edn. Methuen & Co. Ltd, New York. 434 pp.
- Pomeroy, J. W. and Dion, K. 1996. 'Winter radiation extinction and reflection in a boreal pine canopy: measurements and modelling', *Hydrol. Process.*, **10**, 1591–1608.
- Price, A. G. 1988. 'Prediction of snowmelt rates in a deciduous forest', *J. Hydrol.*, **101**, 145–157.
- Price, A. G. and Dunne, T. 1976. 'Energy balance computations in a subarctic area', *Wat. Resour. Res.*, **12**, 686–694.
- Rosenthal, W. 1995. 'Mapping snow cover with automated spectral unmixing', *Trans. AGU EOS* (abstract), **76**, F216.
- Rosenthal, W. and Dozier, J. 1996. 'Automated mapping of montane snow cover at subpixel resolution from the Landsat Thematic Mapper', *Wat. Resour. Res.*, **32**, 115–130.
- Rowe, C. M., Kuiven, K. C., and Jordan, R. 1995. 'Simulation of summer snowmelt on the Greenland ice sheet using a one-dimensional model', *J. Geophys. Res.*, **100**, 16265–16273.
- Sagan, C. and Pollack, J. B. 1967. 'Anisotropic nonconservative scattering and the clouds of Venus', *J. Geophys. Res.*, **72**, 469–477.
- Sellers, P., Hall, F., Margolis, H., Kelly, B., Baldocchi, D., den Hartog, G., Cihlar, J., Ryan, M., Goodison, B., Crill, P., Ranson, K. J., Lettenmaier, D., and Wickland, D. E. 1995. 'The Boreal Ecosystem–Atmosphere Study (BOREAS): an overview and early results from the 1994 field year', *Bull. Am. Meteor. Soc.*, **76**, 1459–1557.
- Shewchuk, S. R. 1997. 'The surface atmospheric sciences mesonet for BOREAS', *J. Geophys. Res.*, **102**, 29077–29082.
- Sturm, M. 1991. 'The role of thermal convection in heat and mass transport in the subarctic snow cover', *CRREL Rep. 91-19*. US Army Corps of Eng., Cold Reg. Res. and Eng. Lab., Hanover.
- Sturm, M. 1992. 'Snow distribution and heat flow in the taiga', *Arctic Alpine Res.*, **24**, 145–152.
- Wiscombe, W. J. and Warren, S. G. 1980. 'A model for the spectral albedo of snow. I, pure snow', *J. Atmos. Sci.*, **37**, 2712–2733.
- Yamazaki, T. and Kondo, J. 1992. 'The snowmelt and heat balance in snow-covered forested areas', *J. Appl. Meteorol.*, **31**, 1322–1327.